Neural Computing and Applications (2020) 32:7995–8010
https://doi.org/10.1007/s00521-019-04267-w

ORIGINAL ARTICLE

Prediction of fresh and hardened properties of self-compacting concrete using support vector regression approach

Prasenjit Saha[1] · Prasenjit Debnath[1] · Paul Thomas[2]

Received: 26 October 2017 / Accepted: 21 May 2019 / Published online: 14 June 2019

Abstract
This article presents the feasibility of using support vector regression (SVR) technique to determine the fresh and hardened properties of self-compacting concrete. Two different kernel functions, namely exponential radial basis function (ERBF) and radial basis function (RBF), were used to develop the SVR model. An experimental database of 115 data samples was collected from different literatures to develop the SVR model. The data used in SVR model have been organized in the form of six input parameters that covers dosage of binder content, fly ash, water–powder ratio, fine aggregate, coarse aggregate and superplasticiser. The above-mentioned ingredients have been taken as input variables, whereas slump flow value, L-box ratio, V-funnel time and compressive strength have been considered as output variables. The obtained results indicate that the SVR–ERBF model outperforms SVR–RBF model for learning and predicting the experimental data with the highest value of the coefficient of correlation (R) equal to 0.965, 0.954, 0.979 and 0.9773 for slump flow, L-box ratio, V-funnel and compressive strength, respectively, with small values of statistical errors. Also, the efficiency of SVR model is compared to artificial neural network (ANN) and multivariable regression analysis (MVR). In addition, a sensitivity analysis was also carried out to determine the effects of various input parameters on output. This study indicates that SVR–ERBF model can be used as an alternative approach in predicting the properties of self-compacting concrete.

Keywords Support vector regression · Kernel functions · Self-compacting concrete · Compressive strength

1 Introduction

Self-compacting concrete (SCC) was first developed in the year 1988, in Japan. Nowadays, SCC is one of the most efficient concrete mixes in the world. Self-compacting concrete is a type of concrete that can flow and fill the formwork without any external forces. Also, it has the ability to consolidate by its own weight. The design mix is mainly focused on two main criteria, namely the requirement of a large amount of finer particle and necessity of high-performing water-reducing admixture. Compared to other traditional concrete, it requires comparatively less human effort which is an added advantage. Also, it increases production rate and reduces noise disturbances. Lot of research studies are being carried out in the area of SCC technology; some of these researches propose better enhancement and durability. Besides all these advantages, SCC has some negative sides. The cost of production of SCC could be 2–3 times higher than ordinary concrete. Therefore, to minimize the cost, some different admixtures such as limestone filler, fly ash (FA), metakaolin, ground-granulated blast-furnace slag (GGBS) and ground clay bricks can be utilized. These ingredients which are used acts as an appropriate substitute for Portland cement [1–7]. To develop SCC three different criteria needed to be fulfilled, such as filling ability, passing ability, segregation resistance. So to meet out these requirements, several trial experiments need to be performed. Lot of questions arises whether SCC is economical and cost-

✉ Prasenjit Saha
pssprasenn@gmail.com

Prasenjit Debnath
prasen458@gmail.com

Paul Thomas
paul.thomas2013@vitalum.ac.in

[1] Department of Civil Engineering, NIT Silchar, Silchar 788010, India

[2] Department of Electrical Engineering, National Institute of Technology, Silchar 788010, India

effective. Another main hurdle is that it is time-consuming to determine the optimum mix. To overcome these limitations, the researchers use a different optimization technique to predict the fresh and hardened properties of concrete.

Sarıdemir [8] developed an artificial neural network (ANN) model to predict compressive strength of concrete containing silica fume and metakaolin. Similar to this, Bilim et al. [9] also proposed a prediction model to estimate the compressive strength of ground-granulated blast-furnace slag concrete. Ozcan et al. [10] performed a comparative study regarding two optimization techniques, namely ANN and fuzzy logic, to forecast compressive strength of silica fume concrete. For similar applications, some of the other researchers also proposed suitable models inspired by Fuzzy and adaptive neuro-fuzzy inference system (ANFIS) to calculate the compressive strength [11–16]. Besides all the advantages of ANN, it has some limitations too, such as poor generalizing performance, slow convergence speed and over-fitting problems. Moreover, to determine the number of hidden layers, there is no specific rule. To overcome these limitations, a new approach, namely support vector machine (SVM) was developed. It renovates and boosts the generalization performance to attain global minimum. Some of the applications using support vector machine technique have been discussed below.

Recently, Sonebi et al. [17] investigated the fresh properties of self-compacting concrete using support vector machine approach. The result was positive and encouraging, which shows better filling ability, flow ability and passing ability. Similar research work was also carried out by different researchers to predict compressive strength of concrete using support vector regression [18–20] and concluded that SVC would be a better and effective model for the forecasting compressive strength of all grades of concrete. Similar to above-mentioned studies, a numerical analysis was carried out by Yan et al. [21] to foreshow elastic modulus for the normal and high strength of concrete using SVM model. Naseri et al. [22] carried out an experimental analysis on SVM-based prediction technique to determine the hardened properties of self-compacting concrete using polypropylene fibre and nano-CuO. Liu [23] discussed the feasibility of using SVM model to determine autogenous shrinkage of concrete mixtures. The SVM model was compared with ANN model to compare its accuracy and efficacy, and the outcomes proved that SVM has the better predicting capability. In another study, Sobhani [24] commented the effectiveness of SVM model to prefigure the strength of no-slump concrete and finally results being contrasted with ANN in his studies. Dong et al. [25] developed a tool to predict acceleration response of nonlinear structure by using support vector machine. From the test results, it was verified that SVM-based model provides better remarkable performance for forecasting and simulation. Amir Saber Mahania et al. [26] employed two optimization techniques, namely particle swarm optimization (PSO) and ant colony optimization, thereafter it was hybridized and compared with weighted least squares support vector machine to determine the optimal shape of the double arch dam. Correspondingly, Yang [27] performed an experimental investigation on corroded reinforced concrete. The experimental result was examined with SVM output. It was noticed that SVM exhibits superior prediction efficiency. SVM can be utilized for wide applications in the field of civil engineering, namely nonlinear structural identification, flood stage forecasting, flood forecasting [28], fracture characteristics of concrete [29], downscaling of precipitation [30], soil improvement, forecasted stream flow and reservoir inflow [31], prediction of groundwater level (GWL) fluctuations [32].

However, most of the research studies on concrete are limited only on predicting the hardened concrete properties. It is also observed from the literature survey that there are no such articles available focusing on prediction of both fresh and hardened properties of self-compacting concrete using support vector regression (SVR) method. Therefore, an effort has been made to predict both fresh and hardened properties of SCC using SVR technique. Also, the efficiency of SVR model is compared to artificial neural network (ANN) and multivariable regression analysis (MVR). An experimental database of 115 samples was collected from the various literatures to develop the SVR model. This study is mainly concentrated on estimating the fresh properties (L-box test, V-funnel test, slump flow)and hardened properties (compressive strength) of SCC from binder content, fly ash, water–powder ratio, fine aggregate, coarse aggregate and superplasticizer as input parameters.

2 Data collection

The main objective of this study is to predict the output parameters related to fresh and hardened properties of SCC. Most of the previous research works are predominately limited to evaluating a single output characteristic of concrete by considering a large number of input variables. Therefore, in this study four output parameters are considered for prediction. The datasets of 115 SCC concrete mix proportions considered for modelling the SVR are presented in Appendix.

The SVR model is designed with six input parameters, namely binder content (B), fly ash percentage (*P*), water–powder ratio (W/B), fine aggregate (F), coarse aggregate (C) and super plasticizer dosage (SP). In the previous studies, modelling was concentrated only on developing

the database from the experimental work; therefore, their database is restricted to a particular variable. In this present study, data are collected from diverse and distinctive source; therefore, it can be applied over to wide applications. In the present study, out of 115 experimental data points, 80% of the data are used to train the SVR model, and the remaining 20% of the data are used to test the model [33]. Statistical parameters of input and output variables used to develop SVR models are enlisted in Table 1.

3 Support vector machine

The support vector machine was first introduced by Vapnik et al. [34]. During the initial stage, it was limited to solve the classification related problems, later it was upgraded to solve regression-related problems also. SVM regression follows the principle of structural risk minimization (SRM) which is much more superior compared to conventional Empirical Risk Minimization (ERM) principle. SRM principle is employed to decline the upper bound generalization error which is very crucial for any statistical learning process. Support vector regression (SVR) is an extension of SVM to solve the prediction- and regression-related problems. Both SVR and SVM use very similar algorithms, but predict different types of variables. The main difference comes in the slack variables used in the two techniques. SVM for classification involves assigning one slack variable to each training data point, whereas in SVM for regression, there are two slack variables for each training data point. In addition to that the main characteristic that differentiates SVR from other model is its ability to improvise generalization performance and to obtain an optimal global solution at the minimum time period. In this paper, Vapnik's ε-insensitive loss function has been used to solve nonlinear regression estimation, and the brief description of SVM regression can be found in Ref. [35, 36].

4 Linear support vector regression

Considering a training dataset $\{(\mathbf{x}_i, y_i), i = 1, 2, 3 \ldots n\}$, where n is the size of training dataset, $\mathbf{x}_i$ is the input vector and y_i is the output vector, respectively. The general linear regression form of SVR can be written as

$$f(\mathbf{x} \cdot \mathbf{w}) = \mathbf{w} \cdot \mathbf{x} + b \tag{1}$$

where $(\mathbf{w} \cdot \mathbf{x})$ indicates the dot product, $\mathbf{w}$ is the weight vector, b is the bias and $\mathbf{x}$ is the test pattern in normalized form. The SRM theory can be performed by reducing empirical risk $R_{emp}(\mathbf{w}, \mathrm{b})$ described as equation, and empirical risk can be defined by using ε-insensitive loss function $L_\epsilon(y_i, f(\mathbf{x_i}, \mathbf{w}))$ indicate as Eq. (3) [34]

$$R_{emp}(\mathbf{w}, \mathbf{b}) = \frac{1}{n}\sum_{i=1}^{n} L_\epsilon(y_i f(\mathbf{x_i}, \mathbf{w})) \tag{2}$$

$$L_\epsilon(y_i, f(\mathbf{x_i}, \mathbf{w})) = \begin{cases} \epsilon, & if\ |y_i - f(\mathbf{x_i}, \mathbf{w})| \le \epsilon \\ |y_i - f(\mathbf{x_i}, \mathbf{w}))| - \epsilon, & otherwise \end{cases} \tag{3}$$

$L_\epsilon(y_i, f(\mathbf{x_i}, \mathbf{w}))$ is the ε-insensitive loss function, or the tolerance error between the target output (y_i) and the estimated output values $f(\mathbf{x_i}, \mathbf{w})$ in optimization process, and $\mathbf{x_i}$ is defined as training pattern. By using ε-insensitive loss function in linear regression problem, the complexity of SVR model can be solved by minimizing $||w||^2$. The deviation of training data outside the ϵ-zone can be estimated by using non-negative slack variable $\left(\xi_i^* \xi_i\right)$.

$$\lim_{w,b,\xi,\xi^*} \left[\frac{1}{2}\mathbf{w} \cdot \mathbf{w} + C\left(\sum_{i=1}^{n} \xi_i^* + \sum_{i=1}^{n} \xi_i\right)\right] \tag{4}$$

Table 1 Statistical parameters of input and output variable

Components	Minimum	Maximum	Average	Reference value	SD	Range
Input variables						
Binder content (kg/m^3)	370	733	523.4	530	71.22173	363
Water–powder ratio	0.26	0.45	0.37	0.37	16.5859	60
Fly ash (%)	0	60	28.7	30	0.060	0.19
Fine aggregate (kg/m^3)	656	1038	852.8	850	89.931	382
Coarse aggregate (kg/m^3)	590	935	742.63	742	121.809	345
Superplasticiser (kg/m^3)	0.74	21.84	8	8	4.669	21.1
Output variables						
D flow (mm)	480	880	660.5	–	56.10818	330
L-box (H_2/H_1)	0.6	1	0.86	–	0.093575	0.4
V-funnel	1.95	19.2	7.75	–	3.844	17.2
Compressive strength (MPa)	10.2	86.8	48.22	–	17.555	69.8

$$\text{Subjected to, } \begin{cases} y_i - w \cdot \mathbf{x}_i - b \le \epsilon + \xi_i^* \\ w \cdot \mathbf{x}_i + b - y_i \le \epsilon + \xi_i, \\ \xi_i^*, \xi_i \ge 0 \end{cases} \quad i = 1, \ldots, n$$

To solve the above-mentioned problem, a saddle point of Lagrange function has to be found

$$\begin{aligned} & L(\mathbf{w}, \xi^*, \xi, \alpha^*, \alpha, C, \gamma^*, \gamma \\ & = \frac{1}{2}\mathbf{w} \cdot \mathbf{w} + c\left(\sum_{i=1}^{n} \xi_i^* + \sum_{i=1}^{n} \xi_i\right) \\ & - \sum_{i=1}^{n} \alpha_i [y_i - \mathbf{w} \cdot \mathbf{x}_i - b + \epsilon + \xi_i] \\ & - \sum_{i=1}^{n} \alpha_i^* \left[\mathbf{w} \cdot \mathbf{x}_i + b - y_i + \epsilon + \xi_i^*\right] \\ & - \sum_{i}^{n} (\gamma_i^* \xi_i^* + \gamma_i \xi_i) \end{aligned} \tag{5}$$

By performing partial differential of Eq. (5) with respect to $\mathbf{w}$, b, $\xi_i^*$and ξ_i, Lagrange function can be minimized by applying Karush–Kuhn–Tucke (KKT) conditions

$$\frac{\partial L}{\partial w} = \mathbf{w} + \sum_{i=1}^{n} \alpha_i \mathbf{x}_i - \sum_{i=1}^{n} \alpha_i^* \mathbf{x}_i = 0; \mathbf{w} = \sum_{i=1}^{n} (\alpha_i^* - \alpha_i)\mathbf{x}_i \tag{6a}$$

$$\frac{\partial L}{\partial b} = \sum_{i=1}^{n} \alpha_i - \sum_{i=1}^{n} \alpha_i^* = 0; \sum_{i=1}^{n} \alpha_i = \sum_{i=1}^{n} \alpha_i^* \tag{6b}$$

$$\frac{\partial L}{\partial \xi^*} = C - \sum_{i=1}^{n} \gamma_i^* - \sum_{i=1}^{n} \alpha_i^* = 0; \sum_{i=1}^{n} \gamma_i^* = C - \sum_{i=1}^{n} \alpha_i^* \tag{6c}$$

$$\frac{\partial L}{\partial \xi} = C - \sum_{i=1}^{n} \gamma_i - \sum_{i=1}^{n} \alpha_i = 0; \sum_{i=1}^{n} \gamma_i = C - \sum_{i=1}^{n} \alpha_i \tag{6d}$$

where the parameter $\mathbf{w}$ of Eq. (6a) is related to parameter w of Eq. (1). After that, putting Eq. (6) into the Lagrange function (5), the dual optimization function can be expressed as

$$\begin{aligned} \max_{\alpha, \alpha^*} [\mathbf{w}(\boldsymbol{\alpha}, \boldsymbol{\alpha}^*)] = \max_{\alpha, \alpha^*} & \left[\sum_{i=1}^{n} y_i (\alpha_i^* - \alpha_i) - \epsilon \sum_{i=1}^{n} (\alpha_i^* - \alpha_i) \right. \\ & \left. - \frac{1}{2} \sum_{ij=1}^{n} (\alpha_i^* - \alpha_i)(\alpha_i^* - \alpha_i)(\mathbf{x}_i \cdot \mathbf{x}_j) \right] \end{aligned} \tag{7}$$

$$\text{subjected to} \begin{cases} \sum_{i=1}^{n} (\alpha_i^* - \alpha_i) = 0, \\ 0 \le \alpha_i^*, \alpha_i \le 0 \end{cases} \quad i = 1, \ldots \ldots n$$

where α_i^* and α_i are defined as Lagrange multiplier [37]. After Solving Eq. (7) with constrains in Eq. (8), the final linear regression function can be expressed as

$$f(\mathbf{x}, \boldsymbol{\alpha}^*, \boldsymbol{\alpha}) = \sum_{i=1}^{n} (a_i^* - a_i)(\mathbf{x}_i \cdot \mathbf{x}) + b \tag{8}$$

5 Nonlinear support vector regression

To solve a complex real-world problem, the linear SVR is not suitable. To perform nonlinear SVR, mapping of input data into high-dimensional feature space is required where linear regression is possible. The input training pattern $\mathbf{x}_i$ is reformed into feature space $\varphi(\mathbf{x}_i)$ by a nonlinear function. After that, the optimization algorithm is applied in the same way as linear SVR. Correspondingly, the nonlinear support vector regression can be expressed as follows

$$f(\mathbf{x}, \mathbf{w}) = \mathbf{w} \cdot \varphi(\mathbf{x}) + b \tag{9}$$

where w and b denote parameter vector and $\varphi(\mathbf{x})$ is used as mapping function from input features to a high-dimensional feature space.

The diagram of nonlinear support vector regression with ε-insensitive loss function is shown in Fig. 1. In the figure, the support vectors are marked with bold points, which have the largest difference from the decision boundary. On the right-hand side of the diagram indicates ε-insensitive loss function, it has an error tolerance ε, upper bound and lower bound are calculated by slack variables (ξ_i^*, ξ_i) . Finally, nonlinear support vector regression can be expressed as

$$\begin{aligned} \max_{\alpha, \alpha^*} [\mathbf{w}(\boldsymbol{\alpha}, \boldsymbol{\alpha}^*)] = \max_{\alpha, \alpha^*} & \left[\sum_{i=1}^{n} y_i (\alpha_i^* - \alpha_i) - \epsilon \sum_{i=1}^{n} (\alpha_i^* + \alpha_i) \right. \\ & \left. - \frac{1}{2} \sum_{ij=1}^{n} (\alpha_i^* - \alpha_i)(\alpha_i^* - \alpha_i)\{\varphi(\mathbf{x}_i) \cdot \varphi(\mathbf{x}_j)\} \right] \end{aligned} \tag{10}$$

$$\text{subjected to} \begin{cases} \sum_{i=1}^{n} (\alpha_i^* - \alpha_i) = 0, \\ 0 \le \alpha_i^*, \alpha_i \le 0 \end{cases} \quad i = 1, \ldots n$$

As the inner product $\varphi(\mathbf{x}_i) \cdot \varphi(\mathbf{x}_j)$ is complex, by using Mercer's condition [38], the inner product can be replaced by using kernel function $\varphi(\mathbf{x}_i) \cdot \varphi(\mathbf{x}_j) = \mathbf{K}(\mathbf{x}_i, \mathbf{x}_j)$.Therefore, Eq. (11) can be written as

$$\begin{aligned} \max_{\alpha, \alpha^*} [\mathbf{w}(\boldsymbol{\alpha}, \boldsymbol{\alpha}^*)] = \max_{\alpha, \alpha^*} & \left[\sum_{i=1}^{n} y_i (\alpha_i^* - \alpha_i) - \epsilon \sum_{i=1}^{n} (\alpha_i^* + \alpha_i) \right. \\ & \left. - \frac{1}{2} \sum_{ij=1}^{n} (\alpha_i^* - \alpha_i)(\alpha_i^* - \alpha_i)\mathbf{K}(\mathbf{x}_i, \mathbf{x}_j)\} \right] \end{aligned} \tag{11}$$

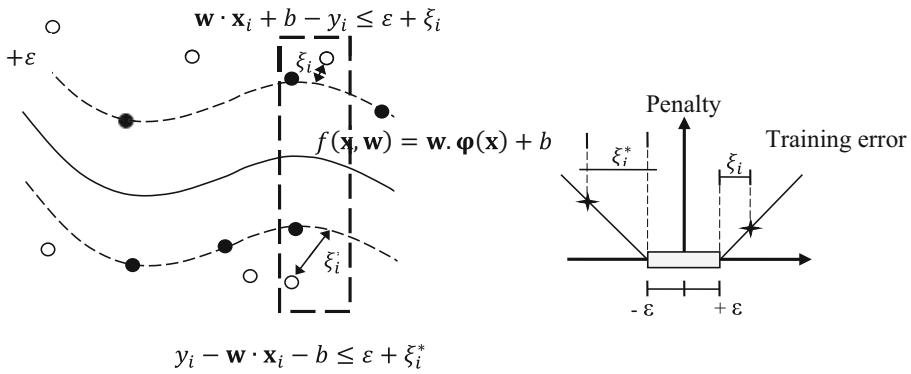

Fig. 1 Nonlinear SVR with insensitive loss function

Table 2 Different types of kernel function

Kernel	Equation
Linear kernel function	$\mathbf{K}(\mathbf{x}_i, \mathbf{x}) = \mathbf{x}_i \cdot \mathbf{x}$
Sigmoid kernel function	$\mathbf{K}(\mathbf{x}_i, \mathbf{x}) = \tanh(a\mathbf{x}_i \cdot \mathbf{x} + b)$
Polynomial kernel function (POLY)	$\mathbf{K}(\mathbf{x}_i, \mathbf{x}) = (\mathbf{x}_i \cdot \mathbf{x} + 1)^d$
Radial basis kernel function (RBF)	$\mathbf{K}(\mathbf{x}_i, \mathbf{x}) = \exp\left(-\mathbf{x}_i - \frac{\mathbf{x}^2}{2\sigma^2}\right)$
Exponential radial basis kernel function (ERBF)	$Kx_i \cdot x = \exp\left(\frac{\sqrt{-x_i - x}}{2\sigma^2}\right)$

σ is the width of RBF and ERBF functions, d is the degree of polynomial function

$$\text{subjected to} \begin{cases} \sum_{i=1}^{n} \left(\alpha_i^* - \alpha_i\right) = 0, \\ 0 \leq \alpha_i^*, \alpha_i \leq 0 \end{cases} \quad i = 1, \ldots n$$

For nonlinear regression, numerous kernel functions have been discussed in the above-mentioned literature. The most commonly used kernel function and their corresponding equations are presented in Table 2. However, in the present study, radial basis and exponential radial basis kernel function have been used. SVR model has been implemented in MATLAB 2013a environment with a support vector machine code [36]. Parameters σ and d are user-defined kernel function. By trial and error, the optimal values of C, ε and kernel parameters are determined [39].

6 Predictive model development

6.1 SVR models development

In order to predict the fresh (L-box ratio, V-funnel, slump flow) and hardened properties of concrete (compressive strength of concrete), nonlinear regression technique was developed through SVR toolbox. Experimental studies indicate that properties of concrete are mostly influenced by binder content (B), fly ash (P), water–powder ratio (W/B), fine aggregate (F), coarse aggregate (C) and superplasticiser dose (SP). Thus, these above-mentioned parameters are taken as an input variable for SVR model, and slump flow (D), L-box ratio, V-funnel, compressive strength (Fc28) are taken as the output variable. These input parameters have different units; hence, the data have to be normalized. After the normalization, the data values lie between the range 0 and 1. To develop the SVR algorithm, several parameters are needed to be determined, namely kernel specific parameters d and σ, error insensitive loss function ε and penalty parameters C. However, the choice of ε and C can be estimated by following some guidelines. The large value of penalty parameter C indicates to minimize the empirical risk which makes the learning algorithm more complicated, on the other hand, the smaller value of penalty parameter C indicates minimization of error within the margin, and this allows learning algorithm with a poor approximation.

The complexity or smoothness of the approximation is influenced by ε parameter. Moreover, it also decides the number of support vector used in final prediction operation. So in order to develop regression function, a smaller value of ε leads to complexities in the learning process having a large volume of support vector, still it would be effective in prediction. On the other hand, the greater value of ε may lead to less number of support vector, resulting in data destruction, which creates flattening in the regression function. However, in the present study, SVR modelling kernel parameter σ and d, loss function parameter ε and penalty parameter C are finalized by trial and error method.

Table 3 (a) SVR model performance with varying C for a constant kernel value and ε. (b) SVR model performance with varying σ for a constant kernel value and ε. (c) SVR model performance with varying ε for a constant kernel value and C

σ	C	ε	R
(a)			
1.1	70	0.00001	0.8971
1.1	60	0.00001	0.9659
1.1	50	0.00001	0.9612
1.1	40	0.00001	0.9599
1.1	30	0.00001	0.959
1.1	20	0.00001	0.9617
1.1	10	0.00001	0.9612
1.1	10	0.00001	0.9612
(b)			
0.1	60	0.00001	0.7439
0.3	60	0.00001	0.8986
0.6	60	0.00001	0.965
0.9	60	0.00001	0.968
1.1	60	0.00001	0.9733
1.3	60	0.00001	0.953
(c)			
1.1	60	0.1	0.873
1.1	60	0.01	0.901
1.1	60	0.001	0.9312
1.1	60	0.0001	0.9521
1.1	60	0.00001	0.9659
1.1	60	0.000001	0.931

6.2 ANN model development

ANN has been used in solving various civil engineering-related problems. For the sake of conciseness, it is restrained to the short discussion of ANN in the present study and can be found in the literature. The input parameter of ANN are considered as dosage of binder content, fly ash, water–powder ratio, fine aggregate, coarse aggregate and superplasticiser, whereas, slump flow value, L-box ratio, V-funnel time and compressive strength have been considered as output variables. The ANN modelling was implemented in MATLAB 2013 software with neural network toolbox. Total 80% experimental data were used for training, and remaining 20% data used for testing the trained model. A feed-forward multilayer perceptron neural network with one hidden layer was adopted. the number of neurons in hidden layer was varied to find the optimum architecture. Optimum architecture of ANN model was characterized by the number of neurons in hidden layer with tan-sigmoid (hyperbolic tangent) transfer function and a pure linear transfer function at output layer. Bayesian regularization back-propagation training algorithm is used for its better generalization to the training data.

6.3 MVR model development

In the present study for the prediction of slump flow value, L-box ratio, V-funnel time and compressive strength of concrete, multivariable regression analysis is also conducted. Here, 80% data are used to develop the MVR model as it was used in ANN model, and rest of 20% data is used to predict the efficiency of the model. A relationship between dependable variable and independable is shown by the following equation:

$$Y = a_0 + a_1x_1 + a_2x_2 + \ldots + a_px_p \pm e$$

where Y is the dependent variable, a_0 is an intercept. a_1, a_2 and a_p are the slopes x_1, x_2 and x_p are independent variables and e is the error. ''a" values are obtained via least square optimization of error.

7 Result and discussion

All models, i.e. SVR, ANN, MVR, has been designed from a dataset of 115 SCC mix proportions. The dosages of binder content, water–powder ratio, fly ash percentage, volume of fine aggregate, volume of coarse aggregate and superplasticiser were varied from 370 to 733 kg/m^3, 0.26 to 0.45, 0 to 60%, 656 to 1038 kg/m^3, 590 to 935 kg/m^3 and 0.74 to 21.84 kg/m^3 respectively. To develop the SVR model, two different kernel function, namely, exponential radial basis kernel and radial basis kernel were considered. Different combinations of d, σ, C and ε were tried on training dataset, and for each combination of these parameters, performance of testing dataset was recorded. Table 3 shows SVR model performance for slump flow prediction with varying C for a constant kernel value and C. Effect of variation in σ on model performance for a constant kernel value and ε is presented in Table 3, and ε variation in models on performance for a constant kernel value and C is presented in Table 3. But due to space limitation, variation in kernel function on the performance of slump flow prediction is only presented here. The dataset of optimum kernel functions of the SVR model for different output parameters is detailed in Table 4.

To evaluate the performance of SVR, ANN, MVR model in predicting the response, different statistical parameters were used, namely coefficient of determination (R^2), mean absolute deviation (MAD), mean square error (MSE), root mean square error (RMSE) and mean absolute percentage error (MAPE). Statistical performance of developed SVR, ANN and MVR model is summarized in Table 5. For predicting the fresh and hardened properties of SCC, exponential radial basis function shows higher degree of accuracy than other prediction model. Due to

Table 4 Value of support vector regression parameters

	Exponential radial basis function			Radial basis function		
	d	C	ε	d	C	ε
Slump flow (mm)	1.1	60	0.00001	0.1	10	0.000001
L-BOX	0.5	1000	0.00001	0.2	130	0.0000001
V-FUNNEL	1.1	10	0.00001	0.1	10	0.00001
Compressive strength	1.1	10	0.00001	0.1	10	0.0001

space limitation, only the best prediction model is discussed.

The slump flow prediction for SVR–ERBF model is presented in Fig. 2. In the Figure, it is clearly demonstrated that all data points are lying within 90% of prediction interval, which confirms that SVR–ERBF model can efficiently use to predict the slump flow. A coefficient of determination 0.931 (MAD = 9.136, MSE = 136.370, RMSE = 11.678 and MAPE = 1.458) was obtained. And also, it suggest that SVR–ERBF model provides better result in slump flow prediction compared to SVR–RBF model (R^2 = 0.590, MAD = 23.040, MSE = 889.769, RMSE = 29.829 and MAPE = 3.494).

The L-box prediction for SVR–ERBF model is shown in Fig. 3. Similarly, for the prediction of L-box ratio, all the predicted data points are lying within 90% interval and coefficient of determination of 0.910 (MAD = 0.018, MSE = 0.001, RMSE = 0.025 and MAPE = 2.105) was achieved for SVR–ERBF model while SVR–RBF model shows lower performance (R^2 = 0.595, MAD = 0.037, MSE = 0.003, RMSE = 0.057 and MAPE = 4.187).

Figure 4 presents the plot of experimental versus predicted values of V-funnel test. For SVR–ERBF model, all the data points are lying within 90% interval with coefficient of determination 0.958 (MAD = 0.488, MSE = 0.523, RMSE = 0.723 and MAPE = 9.381). The SVR–RBF model-based approach shows lower performance (R^2 = 0.595, MAD = 1.402, MSE = 5.581, RMSE = 2.362 and MAPE = 29.437).

The same SVR model was used to predict compressive strength of concrete. After the training process, the model was used to predict the compressive strength. Figure 5 shows the experimental versus predicted compressive strength values with SVR–ERBF model. It can be observed that most of the data points are lying with its bound and its correlation of determination equal to 0.955 (MAD = 2.939,

Table 5 Statistical errors of proposed SVR models

	R^2	MAD	MSE	RMSE	MAPE
Exponential radial basis function					
Slump flow (mm)	0.931	9.136	136.370	11.678	1.458
L-BOX	0.910	0.018	0.001	0.025	2.105
V-FUNNEL	0.958	0.488	0.523	0.723	9.381
Compressive strength	0.955	2.939	14.312	3.783	6.419
Radial basis function					
Slump flow (mm)	0.590	23.040	889.769	29.829	3.494
L-BOX	0.595	0.037	0.003	0.057	4.187
V-FUNNEL	0.595	1.402	5.581	2.362	29.437
Compressive strength	0.284	11.289	228.700	15.123	23.461
ANN					
Slump flow (mm)	0.615	21.982	696.403	26.389	3.469
L-BOX	0.637	0.058	0.004	0.0642	6.382
V-FUNNEL	0.857	1.366	2.738	1.654	19.500
Compressive strength	0.882	5.404	38.464	6.202	11.773
MVR					
Slump flow (mm)	0.135	42.486	2845.13	53.33	6.844
L-BOX	0.649	0.0497	0.003	0.0589	5.491
V-FUNNEL	0.405	2.214	7.223	2.687	40.665
Compressive strength	0.834	5.848	63.705	7.98	14.37

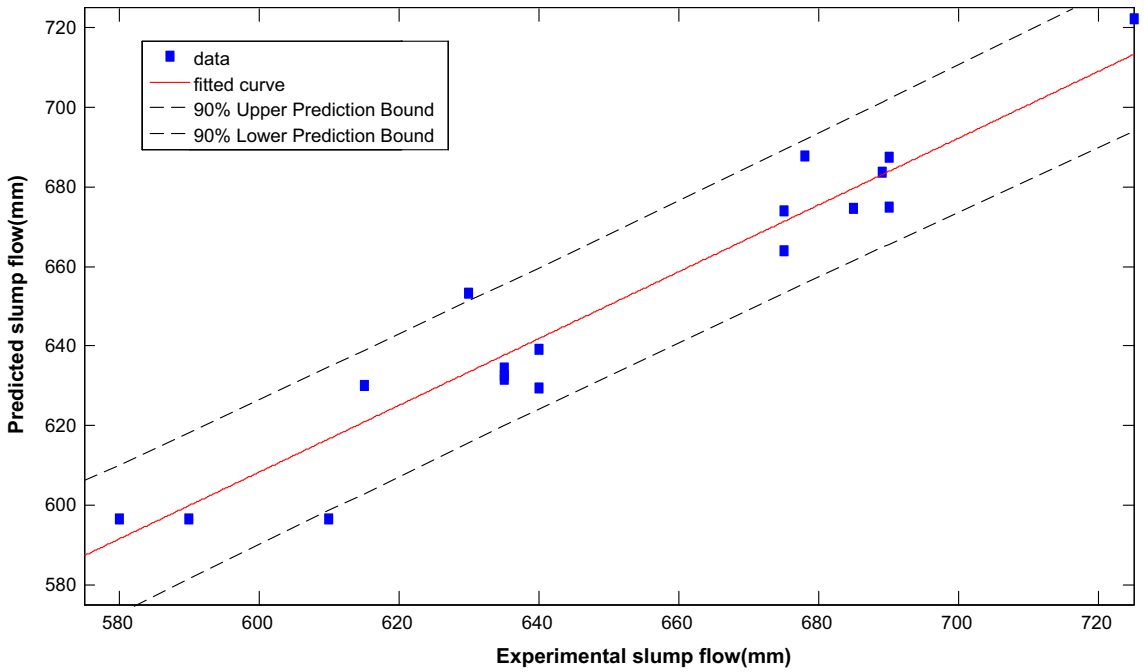

Fig. 2 Experimental versus predicted of slump flow (mm) using SVR–ERBF

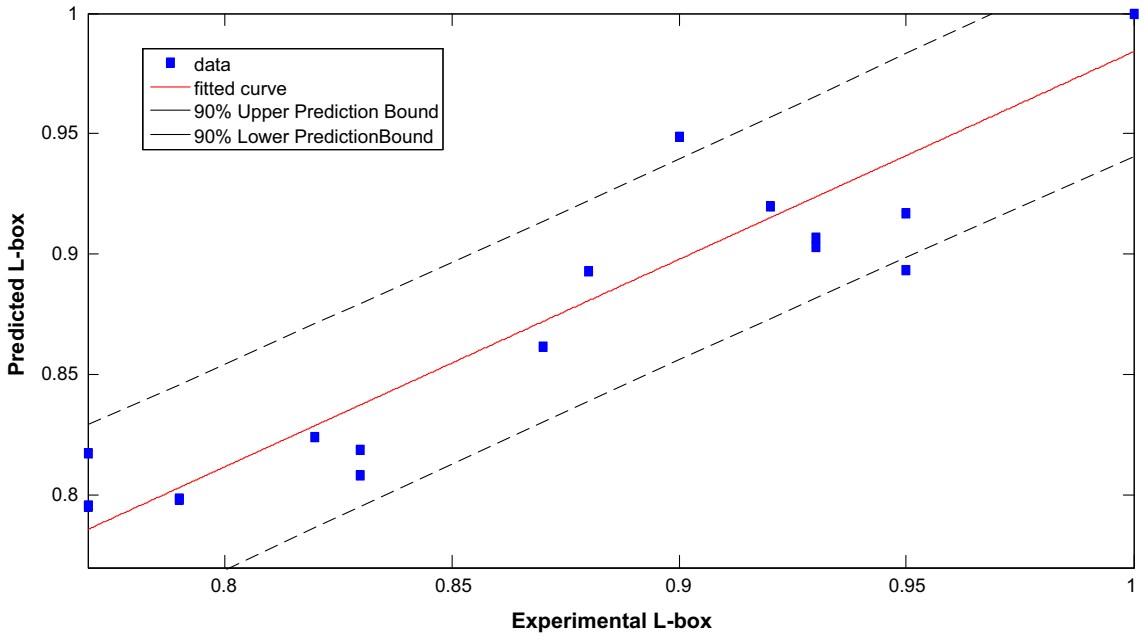

Fig. 3 Experimental versus predicted of L-box using SVR–ERBF

MSE = 14.312, RMSE = 3.783 and MAPE = 6.419) achieved with SVR–ERBF model. Similarly, from the SVR–RBF model, lower performance (MAD = 11.289, MSE = 228.700, RMSE = 15.123 and MAPE = 23.461) is observed.

7.1 Sensitivity analysis results and discussion

A sensitive analysis has been also carried out to obtain the effect the input parameters on output. Therefore, to estimate the effect of input parameters, a particular input parameter is varied within its range with the other

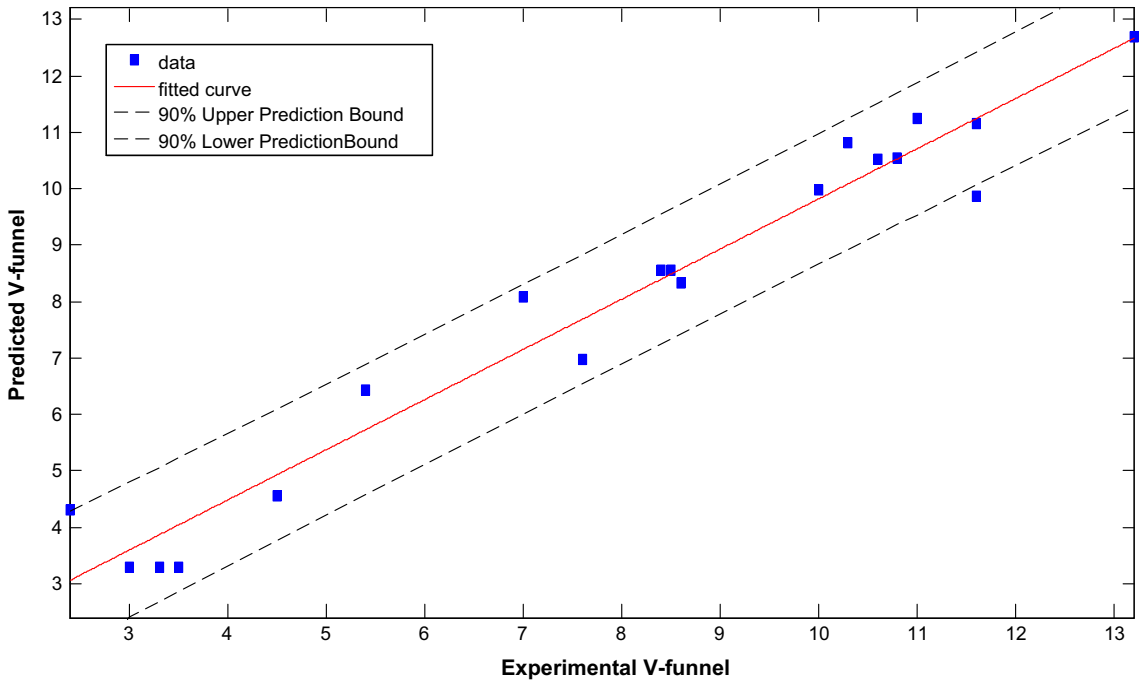

Fig. 4 Experimental versus predicted of V-funnel using SVR–ERBF

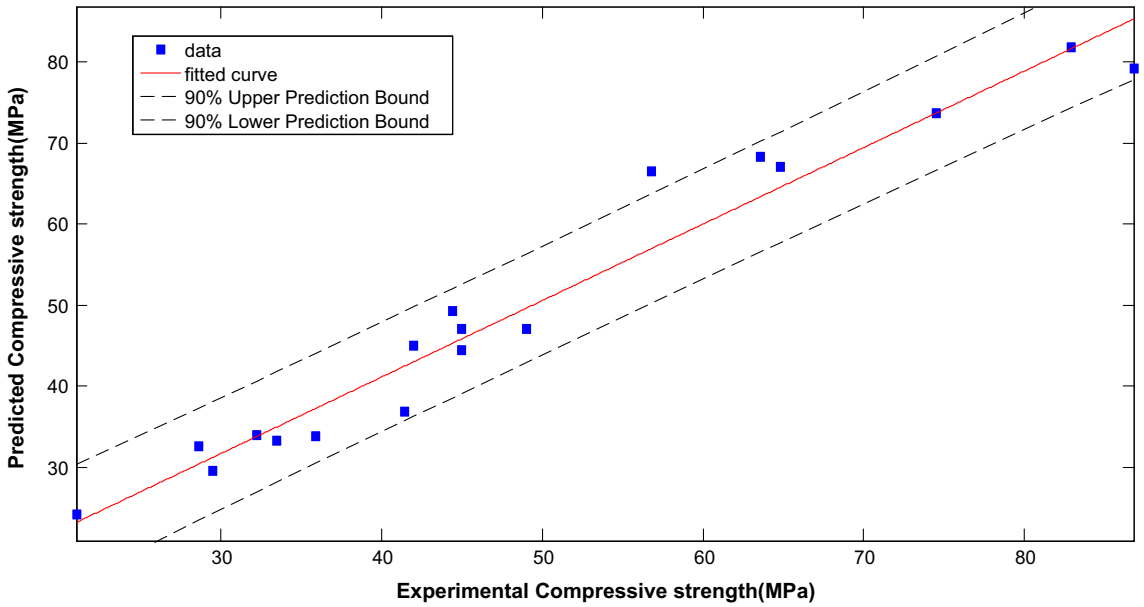

Fig. 5 Experimental versus predicted of compressive strength using SVR–ERBF

parameters being fixed at reference value. Similar procedure is applied for other input parameters to investigate the effect of input parameters on output value. Therefore, the input parameters, i.e. the amount of cement, fly ash, water–powder ratio, fine aggregate, coarse aggregate and Superplasticiser, were varied from 370 to 550 kg/m^3, 0 to 30%, 656 to 846 kg/m^3, 676 to 848 kg/m^3, 600 to 1000 kg/m^3 and 0.74 to 11.24 kg/m^3, respectively.

From Fig. 6, it is clear that the higher concentration of cement, fly ash and fine aggregate content absorbs water causing declination of slump flow diameter. However, increasing the amount of coarse aggregate, water–powder

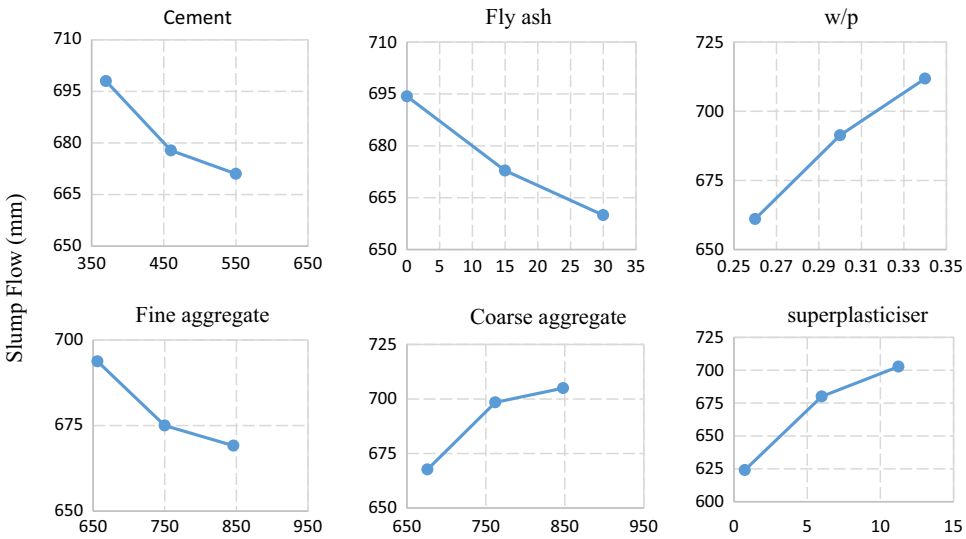

Fig. 6 Sensitivity of mix composition versus slump flow

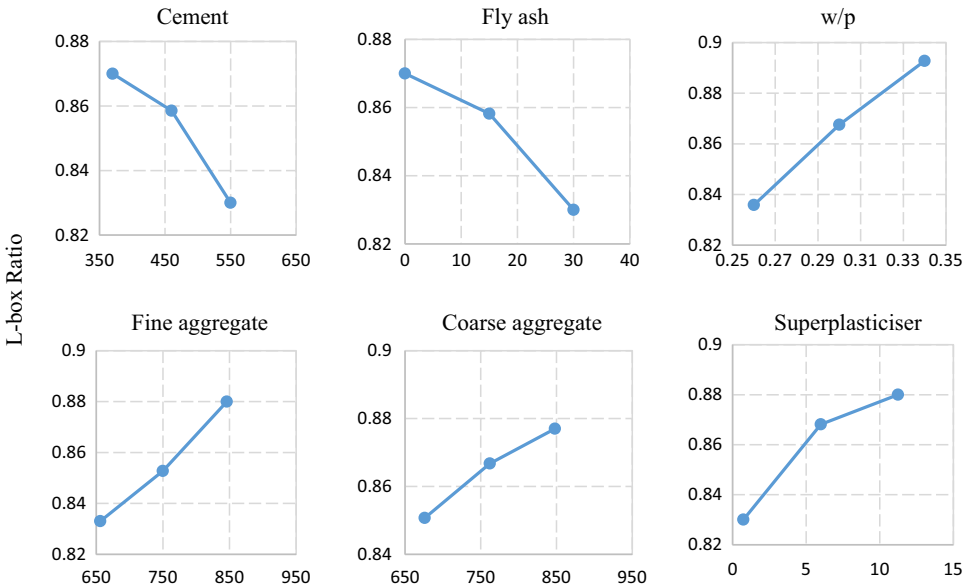

Fig. 7 Sensitivity of mix composition versus L-box ratio

proportion and superplasticiser percentage results in the improvement of slump flow diameter.

From Fig. 7, it can be observed that the increasing water–powder ratio, superplasticiser, fine aggregate, coarse aggregate increases L-box ratio, which reflects better passing ability of SCC. Similarly, an increase in the dosage of powder and fly ash reduces the L-box ratio.

Similarly, to predict the V-funnel time, the same approach has been adopted. Influence of mix composition in predicted V-funnel value is presented in Fig. 8, and it indicates that increase in the amount of water–powder ratio, cement, fly ash, fine aggregate and superplasticiser dosage reduces V-funnel time. Likewise, increase in coarse content increases the V-funnel time.

In Fig. 9, it is illustrated that increasing the amount of cement content enhances compressive strength, and at the same time increase in fly ash percentage reduces the compressive strength. The relationship between water–powder ratio and compressive strength of SCC is also verified from the graph, as decrease in w/p ratio increases compressive strength. Also, it suggests that increase in superplasticiser dosage improves the compressive strength due to the fact that at higher concentration of superplasticiser dosage, requirement of water is less. The plot also indicates that increase in coarse aggregate content improves the hardened property of SCC.

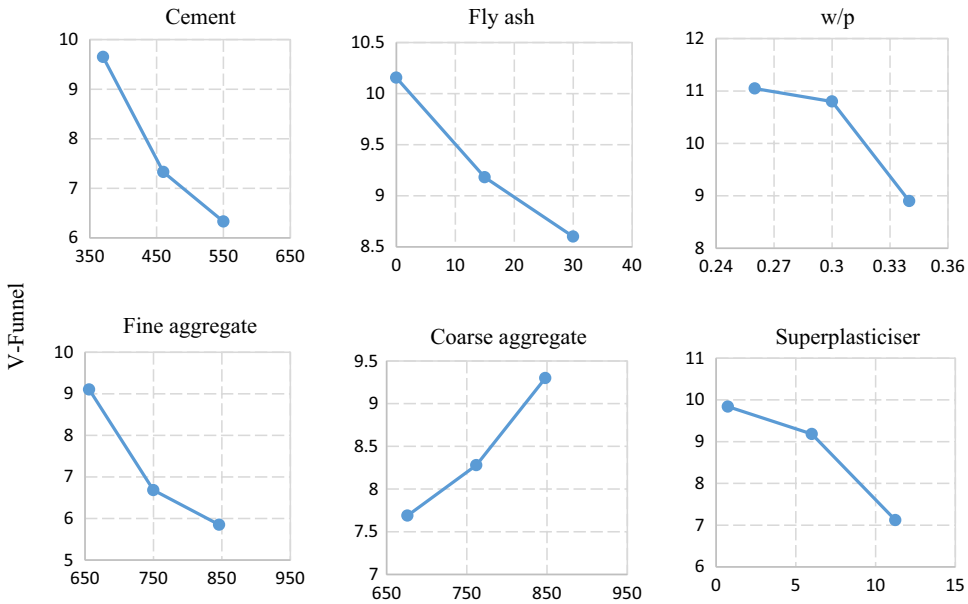

Fig. 8 Sensitivity of mix composition versus V-funnel

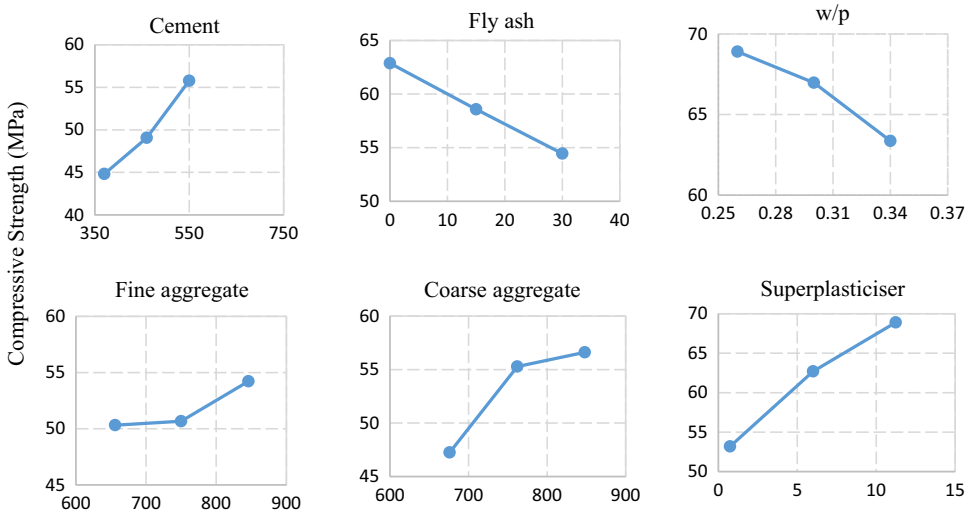

Fig. 9 Sensitivity of mix composition versus compressive strength

8 Conclusions

In this paper, SVR, ANN, MVR approach was used to predict the fresh and hardened properties of self-compacting concrete. Input parameters such as the mix ingredient, namely binder content, fly ash percentage, water–powder ratio, fine aggregate content, coarse aggregate content and superplasticiser, are considered. Based on the study, following conclusions can be drawn.

1. Out of the three prediction model, SVR model with exponential radial basis function yields the best performance based on the highest value of coefficient of correlation of the training and testing data and lowest value of statistical error.
2. Sensitivity analysis shows a clear picture of effect of various input parameters on different outputs parameters, namely slump flow, L-box ratio,V-funnel and compressive strength.
3. This present study represents that the support vector regression technique with exponential radial basis function can be used as a powerful and reliable alternative to solve highly nonlinear problems such as prediction of SCC properties with a high degree of accuracy [40].

Compliance with ethical standards

Conflict of interest The author declares that they have no conflict of interest.

Appendix: Details of experimental variables and test results

Author	Year	*B*	*P*	*W/B*	*F*	*C*	SP	*D* (mm)	L-box	V-funnel	Fc28
Sahmaran et al. [41]	2009	500	0	0.35	1038	639	6.75	665	0.87	12.7	62.2
		500	30	0.34	1006	620	6.75	765	0.95	10.2	52.4
		500	30	0.35	1008	621	6.75	715	0.95	15.8	57.3
		500	40	0.35	995	613	6.75	730	0.85	10.7	59.1
		500	40	0.32	1004	618	6.75	745	0.95	11.7	52.3
		500	50	0.35	988	608	6.75	710	0.9	19.2	40.8
		500	50	0.3	1010	628	6.75	738	0.88	15.1	47.5
		500	60	0.35	979	603	6.75	740	0.85	12.8	38.1
		500	60	0.3	997	614	6.75	770	0.95	9.4	39.9
Siddique [42]	2012	550	15	0.41	910	590	10.45	590	0.95	6.5	29
		550	15	0.41	910	590	10.72	675	0.9	7.5	35.5
		550	20	0.41	910	590	6.6	600	0.7	4.8	24
		550	20	0.41	910	590	7.15	645	0.95	4.5	27
		550	20	0.41	910	590	9.9	605	0.82	7.5	32
		550	20	0.41	910	590	11	690	0.9	4.5	33.5
		550	25	0.42	910	590	7.7	600	0.6	7	26
		550	25	0.42	910	590	8.25	625	0.8	5.2	28
		550	25	0.42	910	590	9.9	605	0.6	7	32
		550	25	0.42	910	590	11	590	0.6	4.2	21.7
		550	30	0.43	910	590	7.15	610	0.87	5.4	21
		550	30	0.43	910	590	7.7	600	0.9	6.5	25.5
		550	30	0.43	910	590	8.8	605	0.7	8.9	27.5
		550	30	0.43	910	590	9.9	675	0.95	5	31
		550	35	0.44	910	590	7.15	590	0.86	6.1	17
		550	35	0.44	910	590	8.8	590	0.8	8	23
		550	35	0.44	910	590	9.35	645	0.9	9	25
		550	35	0.44	910	590	9.9	635	0.92	10	29.5
		500	30	0.35	900	600	11	660	0.9	9	29.2
		500	40	0.35	900	600	10.75	675	0.93	7	28.6
Uysal and Yilmaz [43]	2011	550	25	0.33	887	752	8.8	740	0.93	11.7	73.4
		550	35	0.33	878	742	8.8	750	0.91	17	67.5
		550	15	0.41	910	590	9.9	625	0.82	4	26.5
		550	15	0.41	910	590	10.17	675	0.8	6.6	36
Patel [44]	2003	400	30	0.39	946	900	1.4	510	0.96	4.5	45
		370	36	0.43	960	900	1.85	650	0.94	3	46
		430	36	0.43	830	900	0.86	480	0.6	2.5	36
		430	36	0.43	827	900	2.15	810	0.95	2	48
		400	45	0.45	850	900	1.4	760	1	2.5	38
		400	45	0.39	916	900	1.4	580	1	3	45
		400	45	0.39	916	900	1.4	600	1	3	47
		400	45	0.39	916	900	1.4	570	1	3	49
		400	45	0.39	916	900	1.4	590	1	3.3	49
		400	45	0.39	916	900	1.4	590	1	3.5	49
		400	45	0.39	916	900	2.4	770	1	3.5	43
		450	45	0.39	808	900	1.58	680	1	2.3	50

(continued)

Author	Year	*B*	*P*	*W*/*B*	*F*	*C*	SP	*D* (mm)	L-box	V-funnel	Fc28
		370	54	0.43	930	900	0.74	600	1	2.8	31
		370	54	0.43	928	900	1.85	760	1	2.5	33
		430	54	0.34	874	900	0.86	540	0.87	3.3	46
		430	54	0.36	872	900	2.15	710	1	4	52
		400	60	0.39	886	900	1.4	630	0.91	3.5	44
Gettu et al. [45]	2002	701	37	0.27	774	723	8.1	580	0.8	10	69.5
		733	37	0.26	748	698	8.4	660	0.9	12	68.2
		550	20	0.41	910	590	11.01	690	0.95	4.5	33.2
Siddique et al. [6]	2011	550	25	0.42	910	590	9.91	603	0.85	5.2	31.5
		550	30	0.43	910	590	9.91	673	0.95	6.1	30.7
		550	35	0.44	910	590	9.91	633	0.92	10	29.6
		550	0	0.33	869	778	8.8	690	0.82	14.5	75.9
		550	15	0.33	865	762	8.8	710	0.91	9.4	74.2
Güneyisi et al. [46]	2010	550	0	0.44	826	868	3.5	670	0.71	3.2	61.5
		550	0	0.32	728	935	8.43	670	0.79	17	80.9
		550	20	0.44	813	855	3.2	675	0.71	10.4	52.1
		550	20	0.32	714	917	7.43	730	0.93	7	69.8
		550	40	0.44	801	842	2.96	730	0.8	6	44.7
		550	40	0.32	700	899	7.43	730	0.96	6	60.9
		550	60	0.44	788	829	3	720	0.95	4	30.3
		550	60	0.32	686	881	6.67	730	0.9	7	47.5
		633	0	0.27	656	875	20.58	635	0.79	13.2	86.8
Nepomuceno et al. [47]	2014	643	0	0.29	761	729	19.95	630	0.86	9.9	81.9
		670	0	0.27	695	772	21.84	620	0.81	10.4	85
		551	16	0.31	822	772	11.34	625	0.7	11.6	59.6
		564	16	0.31	841	729	11.55	630	0.77	10.3	56.8
		588	16	0.28	752	820	12.39	635	0.77	11	64.8
		604	16	0.28	772	772	12.71	625	0.8	9.7	63.1
		613	16	0.26	686	875	12.92	615	0.77	12.7	67.5
		618	16	0.28	790	729	13.02	640	0.83	11.6	63.6
		649	16	0.26	726	772	13.65	650	0.84	10	69.1
		613	24	0.26	685	875	15.33	645	0.8	13.3	78.2
		633	24	0.26	706	820	15.86	630	0.79	12.4	79.2
		649	24	0.26	726	772	16.28	655	0.84	10.5	80.3
		567	25	0.3	846	729	13.86	655	0.82	11.3	69.9
		607	25	0.27	774	772	15.12	640	0.83	10.8	74.5
		620	25	0.27	792	729	15.54	635	0.83	10.1	75.7
Bingol and Tohumcu [48]	2013	500	40	0.35	923	663	7.5	680	0.88	6.2	55
		500	55	0.35	908	652	7.5	700	0.91	7	42.7
		450	0	0.45	890	810	9.25	687	0.8	9	50
		480	0	0.4	890	810	13.3	650	0.88	12	52
Krishnapal et al. [49]	2013	450	10	0.45	890	810	8.2	689	0.79	8.6	45
		480	10	0.4	890	810	9.9	665	0.85	9	46
		450	20	0.45	890	810	6.4	690	0.78	8	41
		480	20	0.4	890	810	9.68	685	0.82	8.4	42
		450	30	0.45	890	810	4.8	695	0.78	8	39
		480	30	0.4	890	810	9.4	680	0.8	8.1	40
		575	0	0.31	794	772	17.22	645	0.75	13.3	77.8

(continued)

Author	Year	*B*	*P*	*W/B*	*F*	*C*	SP	*D* (mm)	L-box	V-funnel	Fc28
		589	0	0.31	813	729	17.64	640	0.75	10.6	76.8
		628	0	0.29	744	772	19.53	615	0.77	11.6	82.9
Dhiyaneshwaran et al. [50]	2013	530	20	0.45	768	668	4.55	680	0.95	9.8	37.9
		530	30	0.45	768	668	4.55	690	0.95	8.5	41.4
		530	40	0.45	768	668	4.55	685	0.95	7.9	37.2
		530	50	0.45	768	668	4.55	678	0.95	7.6	35.9
		500	0	0.35	967	694	8	630	0.84	6.1	78.6
		500	25	0.35	938	673	7.5	660	0.85	7	62
Mahalingam and Nagamani [51]	2011	450	30	0.43	789	926	2.77	660	0.88	3.5	44.8
		500	30	0.39	731	862	6.15	640	0.75	2.5	53.6
		550	30	0.35	711	835	4.74	610	0.86	3.2	57.3
		450	40	0.43	780	917	2.77	650	0.88	3.7	41.3
		500	40	0.39	724	850	6.15	680	0.88	2.3	46.7
		550	40	0.35	701	823	6.77	730	0.9	3.4	54.9
		450	50	0.43	770	907	2.5	675	0.72	2.7	37.1
		500	50	0.39	714	836	4.92	730	0.88	2.9	41.8
		550	50	0.35	703	824	5.41	725	0.88	2.4	44.4
		550	15	0.41	910	590	10.73	673	0.89	7.5	35.2
Muthupriya et al. [52]	2012	500	50	0.35	900	600	10.5	680	0.95	7.2	28.7
		530	0	0.45	768	668	4.55	660	0.92	12	30
		530	10	0.45	768	668	4.55	675	0.93	10.6	32.2

References

1. Sfikas IP, Badogiannis EG, Trezos KG (2014) Rheology and mechanical characteristics of self-compacting concrete mixtures containing metakaolin. Constr Build Mater 64:121–129. https://doi.org/10.1016/j.conbuildmat.2014.04.048
2. Beycioglu A, Yilmaz Aruntas H (2014) Workability and mechanical properties of self-compacting concretes containing LLFA, GBFS and MC. Constr Build Mater 73:626–635. https://doi.org/10.1016/j.conbuildmat.2014.09.071
3. Yoo S-W, Ryu G-S, Choo JF (2015) Evaluation of the effects of high-volume fly ash on the flexural behavior of reinforced concrete beams. Constr Build Mater 93:1132–1144. https://doi.org/10.1016/j.conbuildmat.2015.05.021
4. Acharya PK, Patro SK (2015) Effect of lime and ferrochrome ash (FA) as partial replacement of cement on strength, ultrasonic pulse velocity and permeability of concrete. Constr Build Mater 94:448–457. https://doi.org/10.1016/j.conbuildmat.2015.07.081
5. Jalal M, Pouladkhan A, Fasihi O, Jafari D (2015) Comparative study on effects of Class F fly ash, nano silica and silica fume on properties of high performance self compacting concrete. Constr Build Mater 94:90–104
6. Siddique R, Aggarwal P, Aggarwal Y (2012) Influence of water/powder ratio on strength properties of self-compacting concrete containing coal fly ash and bottom ash. Constr Build Mater 29:73–81. https://doi.org/10.1016/j.conbuildmat.2011.10.035
7. Sukumar B, Nagamani K, Srinivasa Raghavan R (2008) Evaluation of strength at early ages of self-compacting concrete with high volume fly ash. Constr Build Mater 22:1394–1401. https://doi.org/10.1016/j.conbuildmat.2007.04.005
8. Saridemir M (2009) Prediction of compressive strength of concretes containing metakaolin and silica fume by artificial neural networks. Adv Eng Softw 40:350–355. https://doi.org/10.1016/j.advengsoft.2008.05.002
9. Bilim C, Atiş CD, Tanyildizi H, Karahan O (2009) Predicting the compressive strength of ground granulated blast furnace slag concrete using artificial neural network. Adv Eng Softw 40:334–340. https://doi.org/10.1016/j.advengsoft.2008.05.005
10. Özcan F, Atiş CD, Karahan O et al (2009) Comparison of artificial neural network and fuzzy logic models for prediction of long-term compressive strength of silica fume concrete. Adv Eng Softw 40:856–863. https://doi.org/10.1016/j.advengsoft.2009.01.005
11. Yaprak H, Karaci A, Demir I (2013) Prediction of the effect of varying cure conditions and w/c ratio on the compressive strength of concrete using artificial neural networks. Neural Comput Appl 22:133–141. https://doi.org/10.1007/s00521-011-0671-x
12. Nazari A, Hajiallahyari H, Rahimi A et al (2012) Prediction compressive strength of Portland cement-based geopolymers by artificial neural networks. Neural Comput Appl. https://doi.org/10.1007/s00521-012-1082-3
13. Riahi S, Nazari A (2012) Predicting the effects of nanoparticles on early age compressive strength of ash-based geopolymers by artificial neural networks. Neural Comput Appl. https://doi.org/10.1007/s00521-012-1085-0
14. Subaşi S, Beycioğlu A, Sancak E, Şahin I (2013) Rule-based Mamdani type fuzzy logic model for the prediction of compressive strength of silica fume included concrete using non-destructive test results. Neural Comput Appl 22:1133–1139. https://doi.org/10.1007/s00521-012-0879-4
15. Kostić S, Vasović D (2015) Prediction model for compressive strength of basic concrete mixture using artificial neural networks. Neural Comput Appl 26:1005–1024. https://doi.org/10.1007/s00521-014-1763-1
16. Belalia Douma O, Boukhatem B, Ghrici M, Tagnit-Hamou A (2016) Prediction of properties of self-compacting concrete

containing fly ash using artificial neural network. Neural Comput Appl 28:707–718. https://doi.org/10.1007/s00521-016-2368-7
17. Sonebi M, Cevik A, Grünewald S, Walraven J (2016) Modelling the fresh properties of self-compacting concrete using support vector machine approach. Constr Build Mater 106:55–64. https://doi.org/10.1016/j.conbuildmat.2015.12.035
18. Lee JJ, Kim DK, Chang SK, Lee J-H (2007) Application of support vector regression for the prediction of concrete strength. Comput Concr 4:299–316
19. Yang HY, Dong YF (2013) Modelling concrete strength using support vector machines. Appl Mech Mater 438–439:170–173. https://doi.org/10.4028/www.scientific.net/AMM.438-439.170
20. Yazdi JS, Kalantary F, Yazdi HS (2013) Prediction of elastic modulus of concrete using support vector committee method. J Mater Civ Eng 25:9–20. https://doi.org/10.1061/(ASCE)MT.1943-5533.0000507
21. Yan K, Shi C (2010) Prediction of elastic modulus of normal and high strength concrete by support vector machine. Constr Build Mater 24:1479–1485. https://doi.org/10.1016/j.conbuildmat.2010.01.006
22. Naseri F, Jafari F, Mohseni E et al (2017) Experimental observations and SVM-based prediction of properties of polypropylene fibres reinforced self-compacting composites incorporating nano-CuO. Constr Build Mater 143:589–598. https://doi.org/10.1016/j.conbuildmat.2017.03.124
23. Liu J, Yan KZ, Zhao X, Hu Y (2016) Prediction of autogenous shrinkage of concretes by support vector machine. Int J Pavement Res Technol 9:169–177. https://doi.org/10.1016/j.ijprt.2016.06.003
24. Sobhani J, Khanzadi M, Movahedian AH (2013) Support vector machine for prediction of the compressive strength of no-slump concrete. Comput Concr 11:337–350. https://doi.org/10.12989/cac.2013.11.4.337
25. Yinfeng D, Yingmin L, Ming L, Mingkui X (2008) Nonlinear structural response prediction based on support vector machines. J Sound Vib 311:886–897. https://doi.org/10.1016/j.jsv.2007.09.054
26. Saber Mahani A, Shojaee S, Salajegheh E, Khatibinia M (2015) Hybridizing two-stage meta-heuristic optimization model with weighted least squares support vector machine for optimal shape of double-arch dams. Appl Soft Comput J 27:205–218. https://doi.org/10.1016/j.asoc.2014.11.014
27. Yang S, Fang CQ, Yuan ZJ (2014) Study on mechanical properties of corroded reinforced concrete using support vector machines. Appl Mech Mater 578–579:1556–1561. https://doi.org/10.4028/www.scientific.net/AMM.578-579.1556
28. Yu PS, Chen ST, Chang IF (2006) Support vector regression for real-time flood stage forecasting. J Hydrol 328:704–716. https://doi.org/10.1016/j.jhydrol.2006.01.021
29. Yuvaraj P, Ramachandra Murthy A, Iyer NR et al (2013) Support vector regression based models to predict fracture characteristics of high strength and ultra high strength concrete beams. Eng Fract Mech 98:29–43. https://doi.org/10.1016/j.engfracmech.2012.11.014
30. Tripathi S, Srinivas VV, Nanjundiah RS (2006) Downscaling of precipitation for climate change scenarios: a support vector machine approach. J Hydrol 330:621–640. https://doi.org/10.1016/j.jhydrol.2006.04.030
31. Lin J-Y, Cheng C-T, Chau K-W (2006) Using support vector machines for long-term discharge prediction. Hydrol Sci J 51:599–612. https://doi.org/10.1623/hysj.51.4.599
32. Yoon H, Jun SC, Hyun Y et al (2011) A comparative study of artificial neural networks and support vector machines for predicting groundwater levels in a coastal aquifer. J Hydrol 396:128–138. https://doi.org/10.1016/j.jhydrol.2010.11.002
33. Debnath P, Dey AK (2017) Prediction of bearing capacity of geogrid-reinforced stone columns using support vector regression. Int J Geomech 18:1–15. https://doi.org/10.1061/(ASCE)GM.1943-5622.0001067
34. Vapnik VN, Golowich SE, Smola A (1996) Support vector method for function approximation, regression estimation, and signal processing. Advances in neural information processing systems, Morgan Kaufmann, San Mateo
35. Vapnik V, Golowich S, Smola A (1997) Support vector method for function approximation, regression estimation, and signal-processing. In: Advances in neural information processing systems. MIT Press, Cambridge, pp 281–287
36. Gunn SR (2001) Support vector machines for classification and regression. In: Technical report. University of Southampton, Southampton. http://www.isis.ecs.soton.ac.uk/isystems/kernel/svm.zip. Accessed 16 May 2018
37. Hillier FS, Editor S, Quantitative C, et al (2008) Linear and Nonlinear Programming. https://doi.org/10.1007/978-0-387-74503-9
38. Vapnik VN, Jordan M, F- J (2000)The nature of statistical learning theory. Springer, New York. ISBN 0-387-98780-0, SPIN 10713304
39. Smola AJJ, Schölkopf B (2004) A tutorial on support vector regression. Stat Comput 14:199–222. https://doi.org/10.1023/B:Stco.0000035301.49549.88
40. Ma CK, Lee YH, Awang AZ et al (2017) Artificial neural network models for FRP-repaired concrete subjected to pre-damaged effects. Neural Comput Appl. https://doi.org/10.1007/s00521-017-3104-7
41. Sahmaran M, Yaman I, Tokyay M (2009) Transport and mechanical properties of self consolidating concrete with high volume fly ash. Cem Concr Compos 31:99–106. https://doi.org/10.1016/j.cemconcomp.2008.12.003
42. Siddique R, Aggarwal P, Aggarwal Y (2011) Prediction of compressive strength of self-compacting concrete containing bottom ash using artificial neural networks. Adv Eng Softw 42:780–786. https://doi.org/10.1016/j.advengsoft.2011.05.016
43. Uysal M, Yilmaz K (2011) Effect of mineral admixtures on properties of self-compacting concrete. Cem Concr Compos 33:771–776. https://doi.org/10.1016/j.cemconcomp.2011.04.005
44. Patel R (2003) Development of statistical models to simulate and optimize self-consolidating concrete mixes incorporating high volume of fly ash. Dissertation, University of Ryerson, Toronto
45. Gettu R, Izquierdo J, Gomes PCC, Josa A (2002) Development of high-strength self-compacting concrete with fly ash: a four-step experimental methodology. In: Proceedings of the 27th conference on our world in concrete and structures, Paramasivam y TH Tan, Singapore, pp 217–224
46. Güneyisi E, Gesolu M, Özbay E (2010) Strength and drying shrinkage properties of self-compacting concretes incorporating multi-system blended mineral admixtures. Constr Build Mater 24:1878–1887. https://doi.org/10.1016/j.conbuildmat.2010.04.015
47. Nepomuceno MCS, Pereira-De-Oliveira LA, Lopes SMR (2014) Methodology for the mix design of self-compacting concrete using different mineral additions in binary blends of powders. Constr Build Mater 64:82–94. https://doi.org/10.1016/j.conbuildmat.2014.04.021
48. Bingol AF, Tohumcu I (2013) Effects of different curing regimes on the compressive strength properties of self compacting concrete incorporating fly ash and silica fume. Mater Des 51:12–18. https://doi.org/10.1016/j.matdes.2013.03.106
49. Krishnapal P, Yadav RK, Rajeev C (2013) Strength characteristics of self compacting concrete containing flyash. Res J Eng Sci. ISSN 2278:9472

50. Dhiyaneshwaran S, Ramanathan P, Baskar I, Venkatasubramani R (2013) Study on durability characteristics of self-compacting concrete with fly ash. Jordan J Civ Eng 7:342–353
51. Mahalingam B, Nagamani K (2011) Effect of processed fly ash on fresh and hardened properties of self compacting concrete. Int J Earth Sci Eng 4(5):930–940. ISSN 0974-5904
52. Muthupriya P, Sri PN, Ramanathan MP, Venkatasubramani R (2012) Strength and workability character of self compacting concrete with GGBFS, FA and SF. Int J Emerg Trends Eng Dev 2(2):424–434. ISSN 2249-6149